Publ. Astron. Soc. Japan 38, 531–545 (1986)

Molecular Line Observations of the S235B Region*

Makoto NAKANO and Shigeomi YOSHIDA

Department of Astronomy, University of Kyoto, Sakyo-ku, Kyoto 606

(Received 1985 June 21; accepted 1986 March 22)

Abstract

The core of the molecular cloud associated with the young stellar object S235B has been observed in molecular lines of CS, CO, and CH_3OH with high angular resolution by the 45-m radio telescope of the Nobeyama Radio Observatory. The core is 0.6×1.0 pc in extent. The number density of molecular hydrogen and the fractional abundance of CS relative to molecular hydrogen are estimated to be $\sim3\times10^5$ cm^{-3} and $\sim5\times10^{-10}$, respectively. Our CO observations show evidence of the bipolar flow. This suggests that S235B is not a compact H II region, but an expanding ionized envelope around a young star. The mass-loss rate from S235B is estimated as $\sim10^{-6}M_\odot$ yr^{-1}. CH_3OH emission shows a very compact distribution and a narrow line width, suggesting that the methanol lines are weakly masing.

Key words: Mass loss; Molecules; Nebulae; Pre-main sequence.

1. Introduction

The S235B region is a star forming complex which contains objects at various evolutionary stages. A young stellar object S235B is located about 10′ south of the classical H II region S235 (Sharpless 1959) and may be the youngest object in this complex. About 1′ north of S235B lies the compact H II region S235A. Other nebulous patches near S235A/B are also reported by several authors (Gyulbudaghian et al. 1978; Cohen 1980). S235B is one of the rare young stellar objects that have been studied at optical as well as infrared and radio wavelengths. Its size is about 10″ on the Palomar Sky Survey red print, corresponding to a linear diameter of 0.1 pc for an assumed distance of 1.8 kpc (Evans and Blair 1981, hereafter EB; Armandroff and Herbst 1981). Optical spectroscopic observations by Glushkov et al. (1975) show a peculiar Hα emission line profile which is characterized by the splitting of the emission line into violet and red components and by broad wings ($-530<V<+370$ km s^{-1}). They considered these features as evidence for violent expanding motion and estimated the electron density to be more than 10^5 cm^{-3}. Israel and Felli (1978) gave an upper limit to the radio continuum emission of 5 mJy at 5 GHz by

* Based on observations made at the Nobeyama Radio Observatory (NRO). NRO, a branch of the Tokyo Astronomical Observatory, University of Tokyo, is a facility open for general use by researchers in the field of astronomy and astrophysics.

aperture synthesis observations. They suggested that the H II region is optically thick at this frequency. The radio continuum observations at 2.7 GHz and infrared observations by Krassner et al. (1982) also support a very high electron density in the core of this source. They considered S235B as an ultracompact H II region. Recently, Ho and Rengarajan (1986) tried to detect the 15-GHz radio continuum flux using the VLA with high spatial resolution ($<1''$). They also give only an upper limit of 0.3 mJy.

In between S235A and B there exists an H_2O maser source (Lo et al. 1975; Genzel and Downes 1977), suggesting the star formation process is still active in this region. S235B is identified as an "intermediate velocity flow source" in a systematic survey for high-velocity molecular outflows associated with young stellar objects by Bally and Lada (1983), and provides with evidence for the mass outflow often associated with the star formation process.

EB have extensively studied the molecular cloud associated with S235 by means of CO molecular lines. The cloud consists of two components: the northern -20 km s^{-1} component which is clearly associated with S235 and the southern -17 km s^{-1} component which contains the compact H II region S235A and S235B. The position of the highest ^{13}CO column density of the southern component coincides with S235B. The existence of the dense molecular cloud core associated with S235A/B was established by their molecular lines and far-infrared observations. The HCN map obtained by Sandell et al. (1983) with $42''$ resolution also shows a maximum intensity near S235B and a sharp decline of intensities toward north and west. Far-infrared observations (Evans et al. 1981) show that the dust temperature rises up to 50 K at S235A and that the 100-μm optical depth is rather large around S235A/B.

The molecular line observations with high spatial resolution are essential to study the dense core of the molecular clouds and to know the direct evidence of the interaction of the young stellar objects and their surrounding molecular medium. In this paper we report a series of new observations of molecular lines with high resolution using the 45-m millimeter-wave telescope of the Nobeyama Radio Observatory (NRO). The observations with CS $J=1$–0, C^{34}S $J=1$–0, CS $J=2$–1, and CH_3OH 8_0–7_1 A^+ lines were made in 1983 and 1984, and $J=1$–0 lines of ^{12}CO and ^{13}CO were observed in 1985. The physical parameters of the core of the molecular cloud are estimated from the observational data. Evidence of the interaction between S235B and the molecular cloud is found. We also report a discovery of a new CH_3OH maser source.

2. Observations

The observing parameters are summarized in table 1. The CS and CH_3OH observations were carried out in April 1983 and March 1984. The CS $J=1$–0 and C^{34}S $J=1$–0 transitions were observed simultaneously using a 35–50-GHz single sideband cooled mixer which covers an instantaneous bandwidth of 2 GHz. A typical system temperature was 500 K. The CS $J=2$–1 and CH_3OH 8_0–7_1 A^+ transitions were observed simultaneously using a 85–115-GHz double sideband cooled mixer which covers 500 MHz with an SSB system temperatures of 600–700 K. The

Table 1. Observing parameters.

Molecule	Transition	Frequency (MHz)	HPBW (arcsec)	Velocity resolution (km s^{-1})
$C^{32}S$	$J=1$–0	48991.0	33	0.23
	$J=2$–1	97981.007	19	0.11
$C^{34}S$	$J=1$–0	48206.948	33	0.23
CH_3OH	$J_K=8_0$–7_1 A$^+$	95169.44	19	0.12
^{12}CO	$J=1$–0	115271.204	14	0.10, 0.65
^{13}CO	$J=1$–0	110201.370	14	0.10, 0.65

main-beam efficiency of the antenna was 0.65 and 0.32 at 49 GHz and 98 GHz, respectively. The ^{12}CO and ^{13}CO $J=1$–0 observations were also carried out in April 1985 with the 45-m telescope at NRO. We used a single sideband cooled mixer receiver which provided a 500-MHz band width. A typical system temperature was 900 K. The main-beam efficiency of the antenna was about 0.3. The radio signals were analyzed using the Acousto-Optical Spectrometer (AOS) system with 16,000 channels in total. The high-resolution AOS, which we used, provides the resolution of 37 kHz corresponding to the velocity resolution of 0.23 km s^{-1}, 0.11 km s^{-1}, and 0.10 km s^{-1} at 49 GHz, 98 GHz, and 115 GHz, respectively. The wide-band AOS, which we used only for CO observations, provides the band width of 250 MHz and the resolution of 250 kHz corresponding to the velocity resolution of 0.65 km s^{-1} at 115 GHz. The half-power beam width of the telescope is 33″ at 49 GHz, 19″ at 98 GHz, and 14″ at 115 GHz.

All observations were made in the position switching mode. The reference position was chosen 20′ away from the source position, well outside the CO cloud associated with S235B (EB). The pointing accuracy of the telescope was better than 10″ in azimuth and elevation, which was secured from observations of 43-GHz SiO maser of U Ori located near the present observational field. The intensity calibration was made with the chopper wheel method. ^{12}CO and ^{13}CO intensities were scaled to those measured toward S235B with the 11-m telescope at Kitt Peak by Thompson et al. (1983) after convolution of our map with their beam. Line intensities are expressed in terms of the T_A^* of Kutner and Ulich (1981), which means antenna temperature corrected for the antenna and atmospheric losses.

3. Results

3.1. CS J=1–0

For the CS lines, the peak intensity, peak velocity, and line width were measured by fitting the spectral lines with a Gaussian profile. The CS $J=1$–0 results are shown in figures 1 and 2 in the form of contour maps of the integrated emission and the peak velocity, respectively. The observed points and the positions of S235A, S235B, and the H_2O maser source are also indicated. The map center (0″, 0″) is at the position of S235B: R.A.=$5^h37^m31^s$, Decl.=+35°39′53″ (1950.0) (Israel and Felli 1978).

The position of the maximum intensity is located 30″ northeast of S235B. The size of the cloud, defined by the half-intensity contour, is about 1′.2×2′.2 in angular

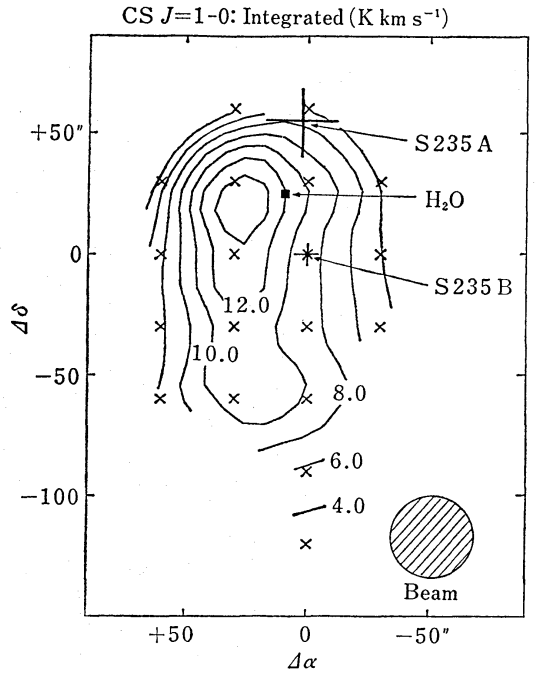

Fig. 1. A contour map of the integrated T_A^* of CS $J=1$–0 emission between -22 and -12 km s^{-1}. Contours are drawn at intervals of 2.0 K km s^{-1}. The half-power beamwidth is also shown. The offsets are in seconds of arc with respect to the position of R.A.$=5^h37^m31^s$, Decl.$=+35°39'53''$ (1950.0). This position corresponds to S235B. Cross marks designate the points where spectra were obtained. The positions of S235A, S235B (Israel and Felli 1978), and the H_2O maser G173.7+2.7 (Genzel and Downes 1977) are indicated.

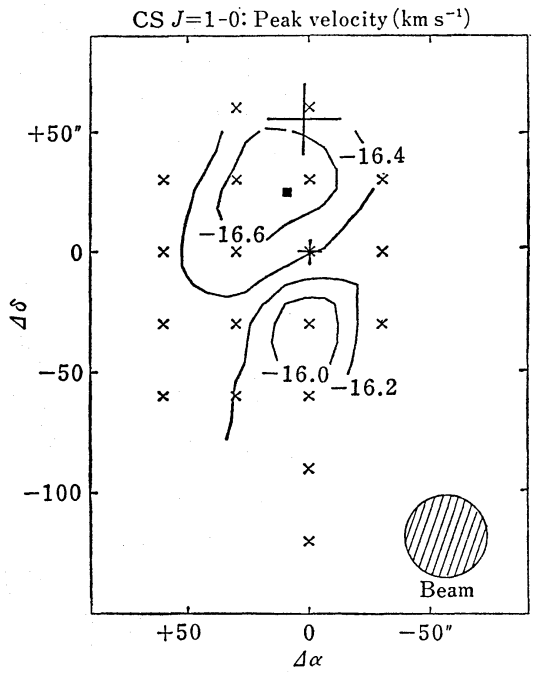

Fig. 2. A contour map of the peak LSR-velocity of the CS $J=1$–0 line. Contours are drawn at intervals of 0.2 km s^{-1}. The other symbols are the same as in figure 1.

extent, which corresponds to 0.6×1.1 pc at the distance of 1.8 kpc. The cloud on the map is apparently extending to the south. This direction nearly coincides with that of the elongated large-scale (~ 10 pc) CO distribution (EB), that of the line connecting nebulous patches, and the direction of the optical interstellar polarization around S235 (Mathewson and Ford 1970). The results of the far-infrared observations with a 37″ beam (Evans et al. 1981) also show that 100-μm optical depths are rather large along the north-south direction. This elongation of the molecular cloud did not appear clearly on the HCN map obtained by Sandell et al. (1983). The HCN intensities sharply drop to the west, while the CS $J=1$–0 line intensities decrease toward northeast. The width of the $J=1$–0 CS line is 2.5 km s^{-1} (FWHM) on the average, and shows no systematic variation over the observed field. The mean velocity is ~ -16.5 km s^{-1}, which agrees well with other molecular line observations by EB. The CS $J=1$–0 profile at the (0″, −60″) position shows velocity components at ~ -16.5 km s^{-1} and ~ -15.5 km s^{-1} blended with each other. The velocity is slightly redshifted to the south of S235B. This may be due to the −15.5 km s^{-1} component in the southern part of the cloud in agreement with the result of HCN observations (Sandell et al. 1983). The $C^{34}S$ $J=1$–0 line is detected with $T_A^* > 0.3$ K at several positions near S235B. The strongest $C^{34}S$ $J=1$–0 emission coincides with the peak of the CS $J=1$–0 line. Line widths are slightly narrower than those of the CS $J=1$–0 transition, and the spatial extent is nearly the same as in figure 1.

3.2. *CS J=2–1 and CH_3OH*

The CS $J=2$–1 and CH_3OH 8_0–7_1 A^+ lines were observed toward 10 positions around the peak of the CS $J=1$–0 emission. Profiles of the CS $J=2$–1 and CH_3OH 8_0–7_1 A^+ sampled every 15″ are shown in figures 3a and 3b, respectively. The highest antenna temperature of the CS $J=2$–1 and CH_3OH emission is observed at the (15″, 15″) position. The profiles of the CS $J=2$–1 line can be approximated by a single Gaussian profile, and are in good agreement with the CS $J=1$–0 profiles in line widths and radial velocities.

As seen in figure 3b, the emission of the CH_3OH line is quite strong at (15″, 15″) and falls off rapidly within 15″ in all directions, suggesting that the size of the source is less than 30″ (<0.26 pc). It is to be noted that there is no sign of emission at the position of S235B (0″, 0″). The observed line width of 0.7 km s^{-1} (FWHM) is much narrower than that of the CS lines (figures 3a and 3b), and the line profile is composed of two velocity features at radial velocities of −16.5 km s^{-1} and −17.5 km s^{-1}. The radial velocity of the stronger component agrees with that of the CS lines.

3.3. *CO*

The ^{12}CO and ^{13}CO observations were carried out at 63 and 9 locations in a grid centered on S235B. The ^{12}CO line profile at S235B is shown in figure 4. The profile shows a prominent wing emission. [The CO line profile by Thompson et al. (1983) toward the same position shows no evidence of wing emission, whereas the wing emission is prominent in a synthesized spectrum made by smoothing our data with a 1′ beam. This could be due to the different coupling to the compact source ($\sim 1'$ in diameter) of the beam of the 11-m telescope and that of the 45-m telescope.] The

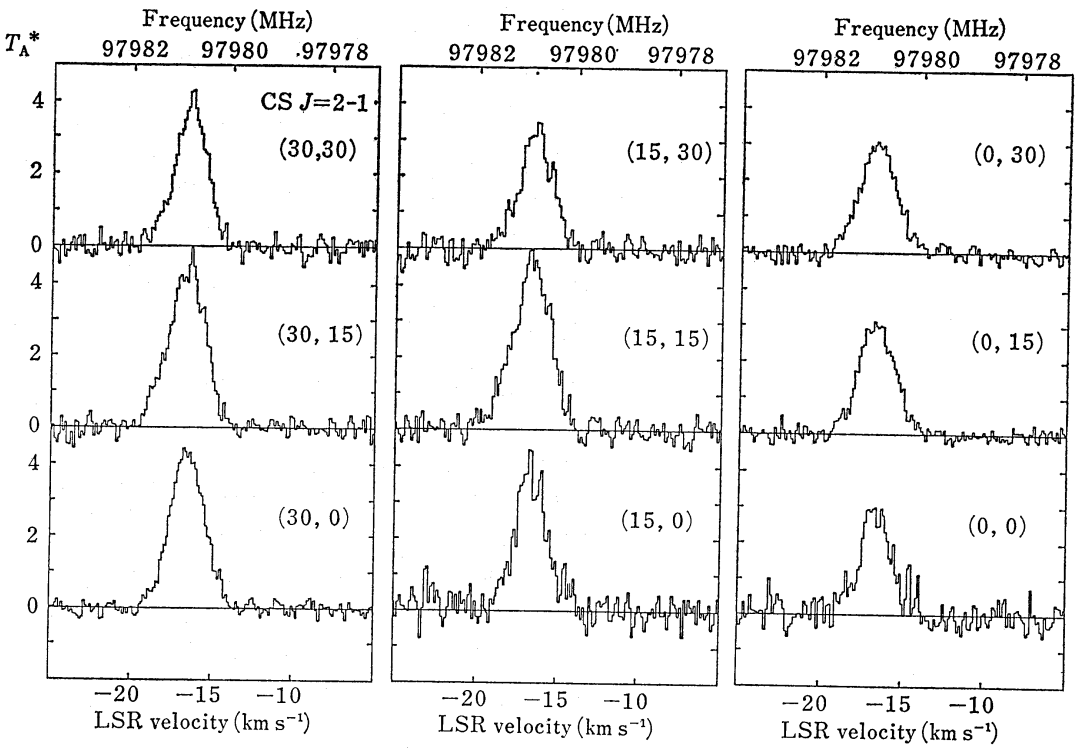

Fig. 3a. The profiles of the CS $J=2$–1 emission sampled every 15″. The numbers in parentheses for each profile give the observed position in arcseconds relative to the position (0″, 0″) of S235B.

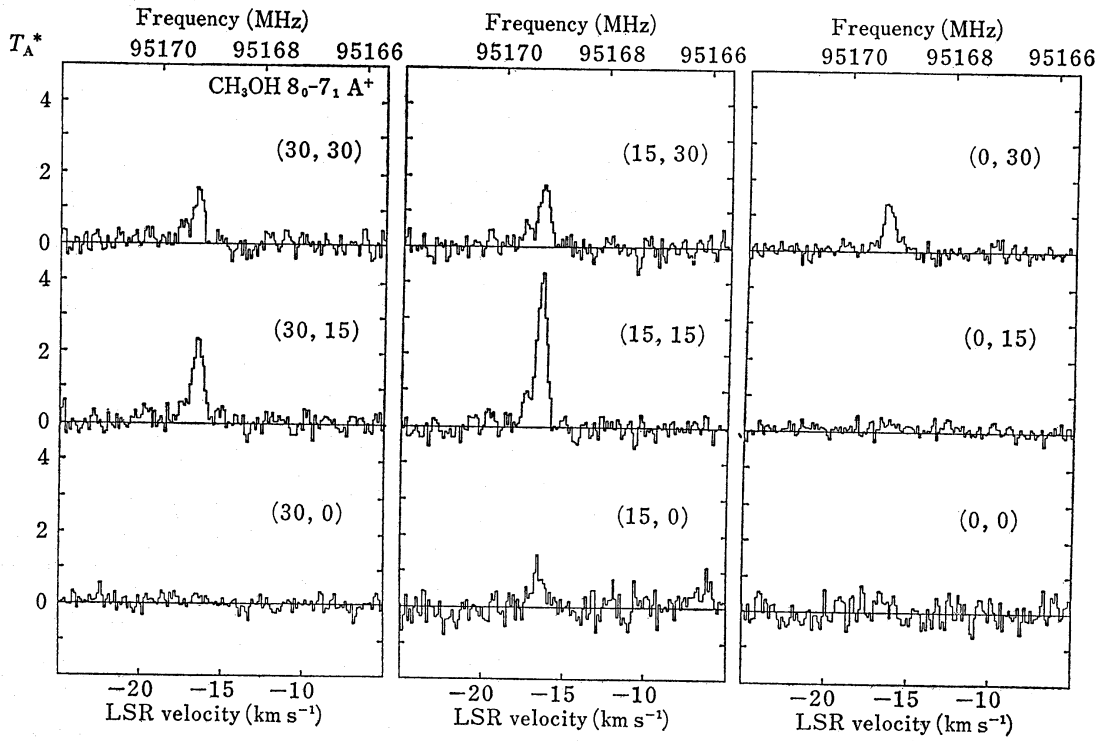

Fig. 3b. Same as figure 3a but for the CH_3OH 8_0–7_1 A^+ emission.

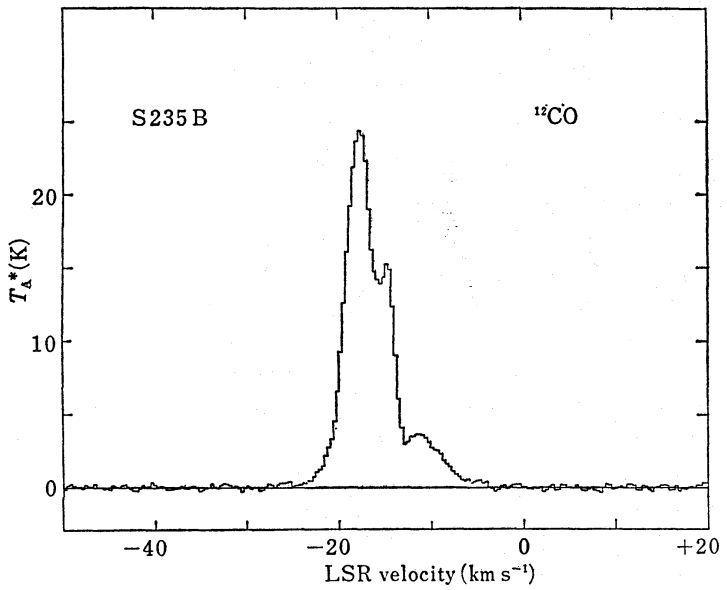

Fig. 4. The profile of the ^{12}CO J=1–0 emission at (0″, 0″).

velocity extent of the wing emission is 22 km s^{-1} consistent with the results obtained by the 7-m telescope at the Bell Laboratories by Bally and Lada (1983). The CS J=1–0 profiles also give the evidence of such wings at (0″, 30″) and (30″, 30″). The ^{12}CO and ^{13}CO profiles at (0″, 15″) and the ^{12}CO profile at (−30″, 0″) are shown in figures 5a and 5b, respectively. Spectrum at (−30″, 0″) shows less prominent blue-shifted line wing. The velocity of the peak emission in the ^{13}CO profiles, −16.0 km s^{-1}, corresponds to the dip in ^{12}CO profiles, as shown in figure 5a. This means that

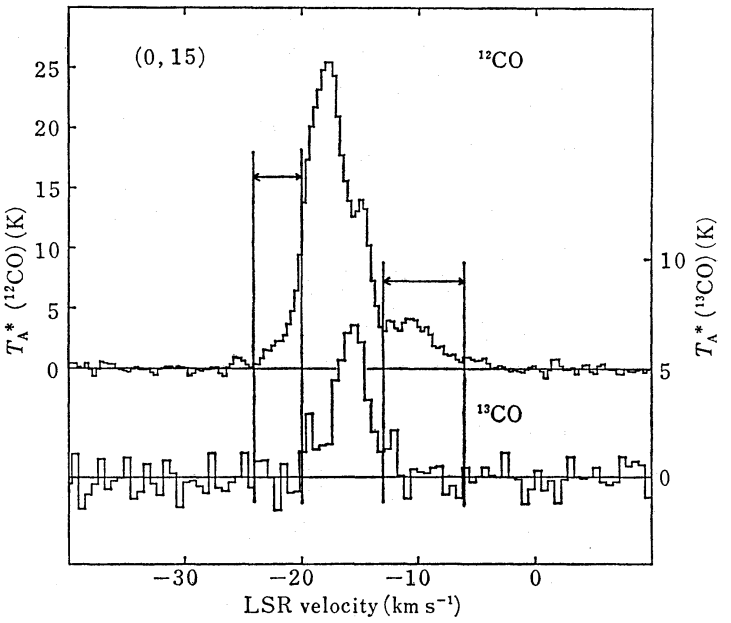

Fig. 5a. The profiles of the CO J=1–0 emission at (0″, 15″). The ^{12}CO and ^{13}CO line profiles are shown with different temperature offsets and scales as shown on both sides of the ordinates. The velocity intervals defined in the text are indicated.

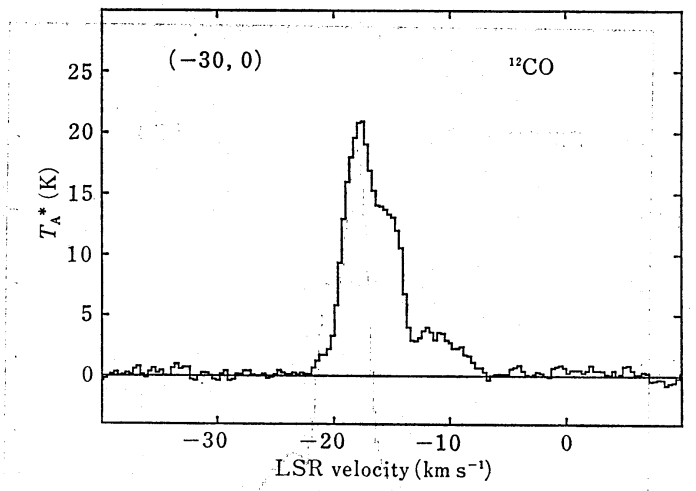

Fig. 5b. The profile of the ^{12}CO $J=1$–0 emission at (−30″, 0″).

this dip is caused by the self-reversal. There also appears a weak feature around −11 km s^{-1} in all our observed spectra. As this feature at −11 km s^{-1} is distributed rather uniformly within our observed area, we consider this as a separate component. Hereafter, we call the −16 km s^{-1} feature and the −11 km s^{-1} feature as the main component and the −11 km s^{-1} component, respectively. The observing points and a contour map of the integrated ^{12}CO intensity of the main component are shown in figure 6.

In order to investigate the distribution of blueshifted high-velocity ^{12}CO emission around S235B, we integrated CO profiles over the velocity from −24 km s^{-1} to −20 km s^{-1}. This velocity interval is determined from ^{12}CO and ^{13}CO spectra and in-

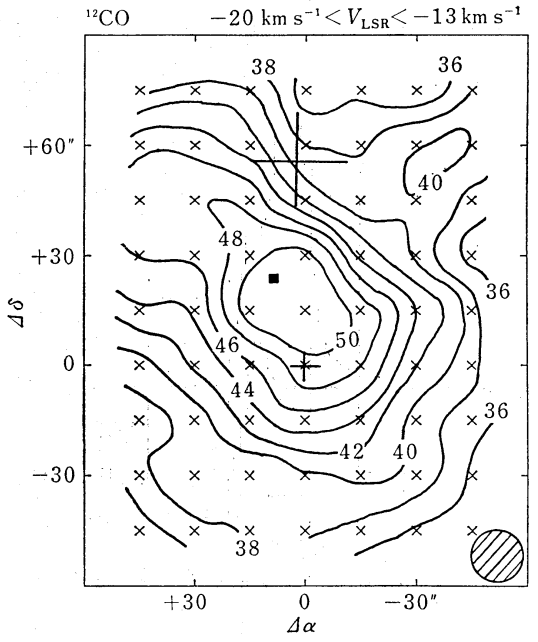

Fig. 6. A contour map of the integrated T_A^* of ^{12}CO $J=1$–0 emission between −20 and −13 km s^{-1} (the main component). The contour unit is 2.2 K km s^{-1}. The other symbols are the same as in figure 1.

dicated in figure 5a. The derived contour map of the blueshifted wing is presented in figure 7a. For comparison, the contour map of the integrated intensity over the velocity from -13 km s^{-1} to -6 km s^{-1} is shown in figure 7b. This velocity interval is also indicated in figure 5a.

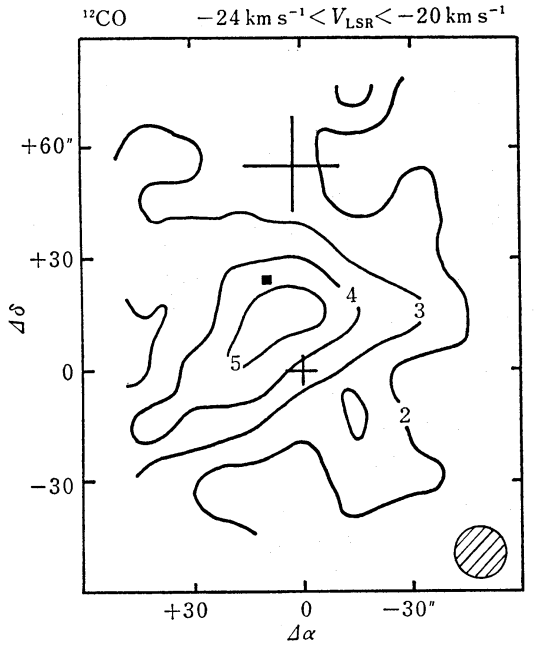

Fig. 7a. A map of the S235B region showing the spatial distribution of the integrated intensity of the ^{12}CO transition over the velocity intervals -24 to -20 km s^{-1} (the blueshifted gas). The contour unit is 2.2 K km s^{-1}. The half-power beamwidth is also shown. Symbols in the map are the same as in figure 1.

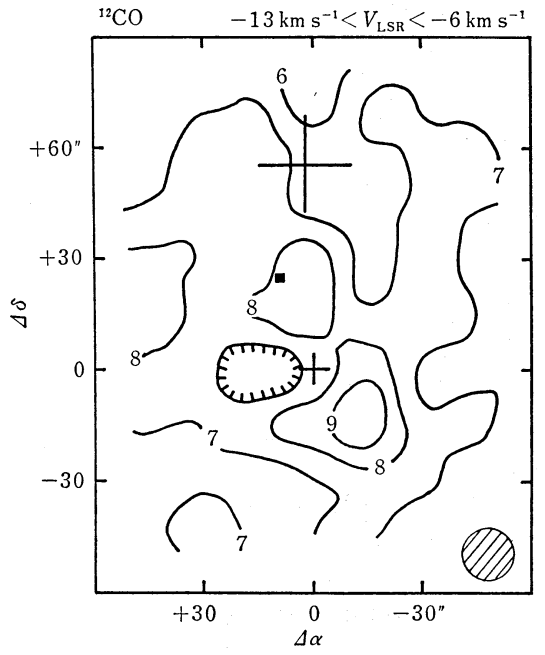

Fig. 7b. Same as figure 7a but for the velocity intervals -13 to -6 km s^{-1} (the -11 km s^{-1} component).

Although the observed area for CO emission is limited, and contaminated with self-reversal, the integrated intensity of CO peaks at the north of S235B (figure 6) coincides with the CS result (figure 1). However, the distribution of CO emission extends to the northeast. The distribution of the blueshifted high-velocity gas is found to be restricted to a region of roughly $30'' \times 30''$ at the northeast of S235B. On the other hand, the integrated intensity of the redshifted emission shown in figure 7b is dominated by the extended -11 km s^{-1} component. However, an increase of the integrated intensity is noticed at the southwest of S235B. This suggests that there exists a redshifted wing, as a counterpart of the blueshifted wing. Thus, these observations can be interpreted in terms of a bipolar structure of the high-velocity gas associated with S235B.

4. Discussion

4.1. The Dense Core

The rotational transitions of carbon monosulfide provide a sensitive probe of high-density regions because of its large dipole moment (Martin and Barrett 1975, 1978). Around the peak of the CS emission, we can determine the space density of this cloud by applying the large-velocity-gradient (LVG) radiative transfer model of Linke and Goldsmith (1980) to the observed intensities of the two transitions of CS lines. By modeling both the source distribution and the beam shape as Gaussians, the antenna-source coupling efficiency is estimated as 0.83 for CS $J=1$–0 and 0.94 for CS $J=2$–1. We have convolved the smaller beam of CS $J=2$–1 into the larger beam of CS $J=1$–0. The kinetic temperature of ~ 25 K has been suggested by the ^{12}CO $J=1$–0 observations (EB; Thompson et al. 1983). Since self-reversal profiles are evident in the CO spectra around S235B, the derived value of 25 K is only a lower limit.

From the derived value of 13 K for $T_R(J=2\text{–}1)$ and 1.6 for $T_R(J=2\text{–}1)/T_R(J=1\text{–}0)$ at (15″, 15″), and assumed T_k, we can estimate $n(H_2)$ and $X(CS)/(dv/dr)$ by figure 3 of Linke and Goldsmith (1980). We find $n(H_2)=4\times10^5$ cm^{-3} and $X(CS)/(dv/dr)=1\times10^{-10}$ (km s^{-1} pc^{-1})$^{-1}$ for $T_k=20$ K, and $n(H_2)=3\times10^5$ cm^{-3} and $X(CS)/(dv/dr)=3\times10^{-10}$ (km s^{-1} pc^{-1})$^{-1}$ for $T_k=40$ K. The choice of the kinetic temperature between 20 K and 40 K will not seriously change these values. If we adopt 2.5 km s^{-1} pc^{-1} as the velocity gradient (EB), we get $X(CS)\sim5\times10^{-10}$, which is in good agreement with those of the other cores of star forming regions studied by Linke and Goldsmith (1980). The total gas density of $(3\text{–}4)\times10^5$ cm^{-3} estimated here is in reasonable agreement with the density estimated by EB from H_2CO observations; $n(H_2)=(5\pm2)\times10^5$ cm^{-3} at (0″, 60″) and $n(H_2)=2\times10^5$ cm^{-3} at (0″, -60″).

Where the C^{34}S has been detected, the CS column density, N(CS), is obtained by assuming that the isotopic ratio is terrestrial, i.e., C^{32}S/C^{34}S=22.6, that C^{34}S has the same excitation temperature as CS, and that all the CS molecules are populated in the local thermodynamic equilibrium. We obtain the optical depth in the CS $J=1$–0 emission of 3.5–7.7, and the excitation temperature of 7–13 K. The peak N(CS) is 1.4×10^{15} cm^{-2} at (30″, 30″) position, and the average over all measurements of N(CS) at 11 positions gives $\langle N(CS)\rangle=9.1\times10^{14}$ cm^{-2}. The column density derived from the

LVG model and that from the LTE assumption agree with each other within a factor of 3.

If we assume that the cloud core, which is approximated as 0.6×1.1 pc in extent and 0.6 pc in thickness, is uniformly filled with a gas of density 3×10^5 cm^{-3}, we can roughly estimate the total mass of the core to be $7\times10^3\,M_\odot$. This value should be regarded as an upper limit to the true mass, since inhomogeneities inside the source will reduce the estimated mass (Snell et al. 1984). Using the average line width over the regions of strong CS emission and the size of 0.6 pc, we obtain a virial mass of $1300\,M_\odot$. If we suppose that the virial mass is applicable, we can get the volume filling factor of dense clumps in the core by comparing the mass estimated from the LVG approximation and the virial mass. The filling factor of 0.2 is thus derived for the core of S235B, in good agreement with those of the S140 and the NGC 2024 molecular clouds (Snell et al. 1984). The total mass of the S235 molecular cloud estimated from ^{13}CO data is $4200\,M_\odot$ (EB), while those of the S140 and NGC 2024 molecular cloud are also $(2\text{–}6)\times10^3\,M_\odot$. This means that more than 20% of the mass is concentrated within the cores of these molecular clouds, which have a volume less than 0.1% of that of the entire molecular clouds.

4.2. The Bipolar Outflow

The present CO maps show that the distribution of the blue- and red-shifted wing emission is displaced in the opposite direction symmetrically about S235B; the blue wing peaks at $\sim20''$ northeast and the red wing peaks at $\sim20''$ southwest of S235B (figures 7a and 7b). This can be interpreted in terms of a bipolar outflow similar to those observed in other young stellar objects. The configuration of the bipolar outflow suggests that the S235B is the source of the outflow.

As the red wing is contaminated with the -11 km s^{-1} component, we treat only the blue wing ($-24\,\mathrm{km\,s^{-1}}<V_{\mathrm{LSR}}<-20\,\mathrm{km\,s^{-1}}$) in the following. If we assume that CO line at the blue wing is optically thin, we can estimate the lower limit of the column density of the outflow. Adopting an LTE condition and $T_{\mathrm{ex}}=20$ K, the derived column density of the outflow is $N(\mathrm{H_2})=2.6\times10^{20}\,\mathrm{cm^{-2}}\times(T_{\mathrm{ex}}/20\,\mathrm{K})$. Following Edwards and Snell (1983) we estimate the outflow parameters from the blueshifted gas, which are given in table 2.

Table 2. Parameters of the blueshifted gas.

Maximum velocity from the line center	8 km s^{-1}
Physical dimension	0.3 pc
Mass	$2M_\odot$
Dynamical time scale	3×10^4 yr
Momentum	$13M_\odot$ km s^{-1}
Momentum supply rate	$4\times10^{-4}M_\odot$ km s^{-1} yr^{-1}
Kinetic energy	1.5×10^{45} erg
Kinetic energy supply rate	$0.4L_\odot$

The energy and momentum supply rates may be compared with those of other outflows driven by stars of similar luminosities. The luminosity of S235B ($\sim10^3L_\odot$) is comparable to those of the infrared sources driving molecular flows in NGC 2071

($750L_\odot$) and GL 490 ($1400L_\odot$). The outflow from S235B is an order of magnitude less massive and two orders of magnitude less energetic than those from such objects. The rate of momentum supply from S235B to the blue wing is comparable to that of the Herbig Be star LkHα 234 (Edwards and Snell 1983), whose luminosity is also $10^3 L_\odot$.

4.3. *The Nature of S235B*

S235B is located not at the peak of the CS intensity but at a marginal position. Assuming an extinction of $A_v=9$ mag for S235B (Tokunaga and Thompson 1979) and a foreground extinction of 2 mag common to that for S235 (Israel and Felli 1978), one is left with 7 mag of extinction associated with S235B itself. Now taking $N(H_2)/A_v=1.25\times10^{21}$ cm^{-2} mag^{-1} (Dickman 1978), one finds $N(H_2)\sim0.9\times10^{22}$ cm^{-2}. This value agrees with the column density of the CO envelope of this molecular cloud (EB). In contrast, the CS column density of the core of the cloud is estimated as $\sim10^{15}$ cm^{-2}, which corresponds to $N(H_2)\sim10^{24}$ cm^{-2}, if we adopt $X(CS)=5\times10^{-10}$. It follows that S235B is embedded in the envelope of the molecular cloud and situated near the front surface of the core of the cloud.

There are two possibilities for the nature of S235B. One is that it is an optically thick H II region. The radio continuum flux of S235B is very weak. The observed upper limits at 2.7, 5, and 15 GHz are an order of magnitude below what is expected for an optically thin H II region on the basis of the data of infrared recombination lines (Israel and Felli 1978; Tokunaga and Thompson 1979; Krassner et al. 1982; Bally and Predmore 1983). The relative weakness of the radio emission may be explained by a model of an optically thick H II region. That is, when an H II region is sufficiently dense and compact, the turning point at which the optical thickness becomes unity shifts to higher frequencies. If we assume that the exciting star is on the main sequence with a spectral type B0 (Krassner et al. 1982) and the initial ambient density is 10^5 cm^{-3} (this paper), the theory of the evolving Strömgren spheres (Spitzer 1978) admits an estimation of the age of the H II region of the order of 3×10^3 yr for an optical radius of 10″ (0.044 pc at 1.8 kpc). An optically thick blackbody in the Rayleigh–Jeans approximation gives the effective blackbody radius, r_{bb}, from the radio continuum flux (Simon et al. 1983). By using the 15-GHz data of Ho and Rengarajan (1986), we obtain $r_{bb}<200$ AU.

A second possible explanation is that S235B is an expanding ionized envelope around the young star (Panagia and Felli 1975). The bipolar CO outflow found in the present observations suggests that the second possibility is more plausible for S235B. Moreover, the large expanding motion of S235B suggested by Glushkov et al. (1975) cannot be explained by the champagne flow of H II regions (Tenorio-Tagle 1979). Recent VLA observations by Turner and Matthews (1984) for several ultracompact H II regions at 2 cm revealed shell or ringlike structure in their core regions. Although the extinction associated with S235B is large, the photographic image of S235B in the Hα reveals no clear evidence of shell structure in its core, rather showing a diffuse halo of about 10″ diameter around the stellar core (Krassner et al. 1982).

If we assume the conservation of momentum between the stellar wind and the

swept interstellar gas, the mass-loss rate can be calculated from our CO observations. Adopting 500 km s^{-1} for the velocity of the stellar wind, which is suggested from Hα profile (Glushkov et al. 1975), we derive $\dot{M}=1\times10^{-6}M_{\odot}$ yr^{-1} for S235B by dividing the momentum supply rate by the velocity of the stellar wind. Mass-loss rate can also be derived from the Brα line flux by using the formula given by Simon et al. (1983). The Brα and Brγ lines of S235B have been observed by Krassner et al. (1982). As Brα/Brγ flux ratio is lower than the intrinsic flux ratio expected from optically thin recombination in a 10^4-K gas, Brα line is suggested to be optically thick. Assuming 500 km s^{-1} as the terminal wind velocity and $A_v=9$ mag, we get $\dot{M}\sim(1\text{–}2)\times10^{-6}M_{\odot}$ yr^{-1} from the Simon et al. [1983, equation (15)] formula which is valid for optically thick Brα line. This mass-loss rate is consistent with our CO result.

4.4. *Maser Emission of CH_3OH*

We have observed the S235B region by the 8_0–7_1 A^+ transition of CH_3OH at 95.2 GHz which was first detected in Orion A (Lovas et al. 1976), and detected it with sufficient intensities. The present observations (figure 3b) suggest that the 8_0–7_1 A^+ line of CH_3OH detected near S235B is the maser emission. The observed characteristics supporting this interpretation are as follows:

1. The spatial distribution of the emission is compact, i.e., less than 0.26 pc.
2. The observed line width of 0.7 km s^{-1} is much narrower than those of any other molecules in this cloud (EB; Sandell et al. 1983; Lafon et al. 1983) except for the H_2O maser emission.
3. There is an H_2O maser source, G173.7+2.7, which is located at (10″, 25″) (Genzel and Downes 1977). If we take into account our pointing accuracy, the positional coincidence between the H_2O maser and the peak CH_3OH emission is fairly good. Lo et al. (1975) originally reported a −21 km s^{-1} component of this H_2O maser at their observing epoch of 1974; then, Blair et al. (1978) detected −4 and −59 km s^{-1} components in 1976. Rodriguez et al. (1980), in the course of monitoring observations of this maser source, found −60, −17, and +4 km s^{-1} components and confirmed its variable nature. The radial velocities of CH_3OH coincide with one of the velocity component of the H_2O maser found by Rodriguez et al. (1980).

CH_3OH maser emission is also expected from the theoretical point of view. Adopting $n(H_2)=1\times10^5$ cm^{-3} and $T_k=40$ K, the large velocity gradient model of CH_3OH, which was applied to the strong maser in Sgr B2 (Morimoto et al. 1985), predicts that a population inversion occurs and that $X(CH_3OH)=(1\text{–}2)\times10^{-8}$ (M. Ohishi, private communication).

A CH_3OH maser has long been known only in the Orion KL region (Barrett et al. 1971; Chui et al. 1974; Hills et al. 1975; Barrett et al. 1975). CH_3OH masers were searched for other sources by Barrett et al. (1971) and Buxton et al. (1977) at 1 cm, but with a negative result. Gottlieb et al. (1979) observed CH_3OH by its $J=2$–1 transitions at 96.7 GHz toward 14 galactic sources. They explained these emissions as optically thin cases except for Sgr B2.

Recently new CH_3OH masers were reported from various transitions and sources. These are the 9_2–10_1 A^+ transition from W3(OH) and NGC 7538–IRS 1 (Wilson et al. 1984), the 4_{-1}–3_0 E transition from Sgr B2 and the 7_0–6_1 A^+ transition from Sgr B2,

W51, G13.66−0.60, and G30.82−0.06 (Morimoto et al. 1985), and the 2_1–3_0 E transition from W3(OH) (Wilson et al. 1985). We found that S235A/B is another CH_3OH source, and the 8_0–7_1 A^+ transition is also masing. It is a characteristic common to other maser sources. Furthermore, it is located near the H_2O maser and the dense core of the molecular cloud. The methanol abundance is an order of magnitude larger than the value derived for the extended methanol emission of Orion A (Gottlieb et al. 1979).

5. Summary

We observed the molecular cloud core associated with S235B. Our CS observations show that the cloud has an elongated structure, with an orientation very close to that of the chain of nebulous objects in the Hα emission. The density of the core is estimated to be 3×10^5 cm^{-3} from an analysis of the CS J=1–0 and J=2–1 lines based on the large velocity gradient model. The fractional abundance of CS agrees with those in the cores of giant molecular clouds studied by Linke and Goldsmith (1980). The filling factor of 0.2 is also derived for the core. We obtained a high-resolution CO map of the S235B region. ^{12}CO profiles revealed evidence of an bipolar flow, which suggests that S235B is the source of mass outflow. The mass-loss rate of S235B estimated from our CO observations is $\sim10^{-6}M_\odot$ yr^{-1}.

CH_3OH 8_0–7_1 A^+ line detected near the H_2O maser is characterized by a small line width and a compact spatial distribution. This suggests that the methanol line is weakly masing.

The authors wish to express their hearty thanks to the staff members of the Nobeyama Radio Observatory, especially to Dr. Tetsuo Hasegawa for his valuable comments. They thank Dr. Masatoshi Ohishi for providing his unpublished results of a statistical equilibrium calculation of CH_3OH. They would also like to thank Professor Tomokazu Kogure for his constant encouragement and critical reading of the manuscript. One of the authors (M. N.) acknowledges his gratitude to the Japan Society for the Promotion of Science for financial aid. The data processing was carried out with the FACOM-M200 at NRO.

References

Armandroff, T. E., and Herbst, W. 1981, *Astron. J.*, **86**, 1923.
Bally, J., and Lada, C. J. 1983, *Astrophys. J.*, **265**, 824.
Bally, J., and Predmore, R. 1983, *Astrophys. J.*, **265**, 778.
Barrett, A. H., Ho, P., and Martin, R. N. 1975, *Astrophys. J. Letters*, **198**, L119.
Barrett, A. H., Schwartz, P. R., and Waters, J. W. 1971, *Astrophys. J. Letters*, **168**, L101.
Blair, G. N., Davis, J. H., and Dickinson, D. F. 1978, *Astrophys. J.*, **226**, 435.
Buxton, R. B., Barrett, A. H., Ho, P. T. P., and Schneps, M. H. 1977, *Astron. J.*, **82**, 985.
Chui, M. F., Cheung, A. C., Matsakis, D., Townes, C. H., and Cardiasmenos, A. G. 1974, *Astrophys. J. Letters*, **187**, L19.
Cohen, M. 1980, *Astron. J.*, **85**, 29.
Dickman, R. L. 1978, *Astrophys. J. Suppl.*, **37**, 407.
Edwards, S., and Snell, R. L. 1983, *Astrophys. J.*, **270**, 605.

Evans, N. J., II, Beichman, C., Gatley, I., Harvey, P., Nadeau, D., and Sellgren, K. 1981, *Astrophys. J.*, **246**, 409.
Evans, N. J., II, and Blair, G. N. 1981, *Astrophys. J.*, **246**, 394 (EB).
Genzel, R., and Downes, D. 1977, *Astron. Astrophys. Suppl.*, **30**, 145.
Glushkov, Yu. I., Denisyuk, E. K., and Karyagina, Z. V. 1975, *Astron. Astrophys.*, **39**, 481.
Gottlieb, C. A., Ball, J. A., Gottlieb, E. W., and Dickinson, D. F. 1979, *Astrophys. J.*, **227**, 422.
Gyulbudaghian, A. L., Glushkov, Yu. I., and Denisyuk, E. K. 1978, *Astrophys. J. Letters*, **224**, L137.
Hills, R., Pankonin, V., and Landecker, T. L. 1975, *Astron. Astrophys.*, **39**, 149.
Ho, P. T. P., and Rengarajan, T. N. 1986, in *Star Forming Regions, IAU Symp. No. 115*, ed. M. Peimbert and J. Jugaku (Reidel, Dordrecht), in press.
Israel, F. P., and Felli, M. 1978, *Astron. Astrophys.*, **63**, 325.
Krassner, J., Pipher, J. L., Sharpless, S., and Herter, T. 1982, *Astron. Astrophys.*, **109**, 223.
Kutner, M. L., and Ulich, B. L. 1981, *Astrophys. J.*, **250**, 341.
Lafon, G., Deharveng, L., Baudry, A., and de La Noë, J. 1983, *Astron. Astrophys.*, **124**, 1.
Linke, R. A., and Goldsmith, P. F. 1980, *Astrophys. J.*, **235**, 437.
Lo, K. Y., Burke, B. F., and Hashick, A. D. 1975, *Astrophys. J.*, **202**, 81.
Lovas, F. J., Johnson, D. R., Buhl, D., and Snyder, L. E., 1976, *Astrophys. J.*, **209**, 770.
Martin, R. N., and Barrett, A. H. 1975, *Astrophys. J. Letters*, **202**, L83.
Martin, R. N., and Barrett, A. H. 1978, *Astrophys. J. Suppl.*, **36**, 1.
Mathewson, D. S., and Ford, V. L. 1970, *Mem. Roy. Astron. Soc.*, **74**, 139.
Morimoto, M., Ohishi, M., and Kanzawa, T. 1985, *Astrophys. J. Letters*, **288**, L11.
Panagia, N., and Felli, M. 1975, *Astron. Astrophys.*, **39**, 1.
Rodriguez, L. F., Moran, J. M., Ho, P. T. P., and Gottlieb, E. W. 1980, *Astrophys. J.*, **235**, 845.
Sandell, G., Höglund, B., and Kislyakov, A. G. 1983, *Astron. Astrophys.*, **118**, 306.
Sharpless, S. 1959, *Astrophys. J. Suppl.*, **4**, 257.
Simon, M., Felli, M., Cassar, L., Fischer, J., and Massi, M. 1983, *Astrophys. J.*, **266**, 623.
Snell, R. L., Mundy, L. G., Goldsmith, P. F., Evans, N. J., II, and Erickson, N. R. 1984, *Astrophys. J.*, **276**, 625.
Spitzer, L., Jr. 1978, *Physical Processes in the Interstellar Medium* (John Wiley and Sons, New York), p. 246.
Tenorio-Tagle, G. 1979, *Astron. Astrophys.*, **71**, 59.
Thompson, R. I., Thronson, H. A., Jr., and Campbell, B. 1983, *Astrophys. J.*, **266**, 614.
Tokunaga, A. T., and Thompson, R. I. 1979, *Astrophys. J.*, **233**, 127.
Turner, B. E., and Matthews, H. E. 1984, *Astrophys. J.*, **277**, 164.
Wilson, T. L., Walmsley, C. M., Menten, K. M., and Hermsen, W. 1985, *Astron. Astrophys.*, **147**, L19.
Wilson, T. L., Walmsley, C. M., Snyder, L. E., and Jewell, P. R. 1984, *Astron. Astrophys.*, **134**, L7.